Intermetallics 18 (2010) 1498–1506

Contents lists available at ScienceDirect

Intermetallics

journal homepage: www.elsevier.com/locate/intermet

The 400 °C isothermal section of the Mg–Al–Ca system

D. Kevorkov [a], M. Medraj [a,*], Jian Li [b], E. Essadiqi [b], P. Chartrand [c]

[a] Department of Mechanical Engineering, Concordia University, Montreal H3G 1M8, Canada
[b] Materials Technology Laboratory, CANMET, 568 Booth Street, Ottawa, Canada
[c] Centre for Research in Computational Thermochemistry, Department of Chemical Engineering, Ecole Polytechnique, Montreal, Canada

ARTICLE INFO

Article history:
Received 21 July 2009
Received in revised form
27 February 2010
Accepted 31 March 2010
Available online 24 April 2010

Keywords:
A. Ternary alloy systems
B. Phase diagram
B. Phase identification
F. Diffraction
F. Electron microprobe

ABSTRACT

The Mg–Al–Ca system is experimentally investigated at 400 °C using diffusion couples and key experiments. Phase relations and solubility limits were determined for binary and ternary phases using EPMA and XRD techniques. The Mg_2Ca, $(Al,Mg)_2Ca$ phases were found to form substitutional solid solutions where Al substitutes Mg atoms. The $Al_2(Mg,Ca)$ and $Al_{140}Mg_{89}$ phases form solid solutions where Ca substitutes Mg atoms. The Al_2Ca phase has a complex solid solution where Mg substitutes both Al and Ca atoms. No ternary solubility was found for the Al_4Ca phase. Based on the results of the phase analysis and experimental literature data, the isothermal section of the Mg–Al–Ca phase diagram at 400 °C has been constructed.

1. Introduction

Mg-alloys attract attention of the automotive and aerospace industries because they can help to achieve a significant weight reduction and a higher fuel efficiency compared to steel and aluminum alloys. Recent research showed that Ca can replace the expensive rare-earth metals in the creep resistant Mg–Al–RE alloys used for high-temperature applications [1]. It is also known that Ca could be used as a grain-refining addition to AZ or AM alloys [2].

Several experimental studies and thermodynamic models of the Mg–Al–Ca system were published during last decade. However, numerous discrepancies on the compositions of ternary phases and solid solutions were noticed in the literature. Therefore, additional experimental study of the Mg–Al–Ca phase diagram is essential for understanding the phase relations in this system at elevated temperatures.

Four Laves phases were reported in the Mg–Al–Ca system. The Mg_2Ca-C14 and Al_2Ca-C15 Laves phases demonstrate extensive ternary solubilities. The ternary solubility ranges and their temperature dependence is still not determined exactly. The most diverse information could be found on the composition and homogeneity ranges of the $(Al,Mg)_2Ca$-C36 Laves phase. It is also reported by Suzuki et al. [3,4] that $(Al,Mg)_2Ca$ is a high temperature phase, but the exact decomposition temperature was not determined. The second ternary C36 Laves phase with a $Al_2(Mg,Ca)$ composition was reported by Zhong et al. [5]. Its stability and solubility range should be verified.

The aim of the present work is to determine the compositions and solubility ranges of the Laves phases in the Mg–Al–Ca system at 400 °C and to construct the isothermal section of the Mg–Al–Ca phase diagram at 400 °C.

2. Literature review

The Al–Mg–Ca phase diagram has been studied by several authors [2–17]. Catterall et al. [6] studied the system experimentally and reported a partial isothermal section of the Mg-rich corner. The complete phase diagram was constructed by Gröbner et al. [7] using thermodynamic modeling and key experiments. The isothermal section of this system at 400 °C is shown in Fig. 1 (a). A thermodynamic model was constructed by [7] after XRD, SEM/EDS and DTA study of twenty-five alloys. They reported wide solubility ranges for the Mg_2Ca, Al_2Ca and Al_3Ca_8 solid solutions and mentioned that the ternary solid solubilities do not vary substantially with temperature. No ternary phases were reported.

Ozturk et al. [8,9] published an experimental study and a thermodynamic model of the Mg–Al–Ca ternary system, but two

* Corresponding author.
E-mail address: mmedraj@encs.concordia.ca (M. Medraj).
URL: http://users.encs.concordia.ca/~mmedraj

0966-9795/$ – see front matter © 2010 Elsevier Ltd. All rights reserved.
doi:10.1016/j.intermet.2010.03.038

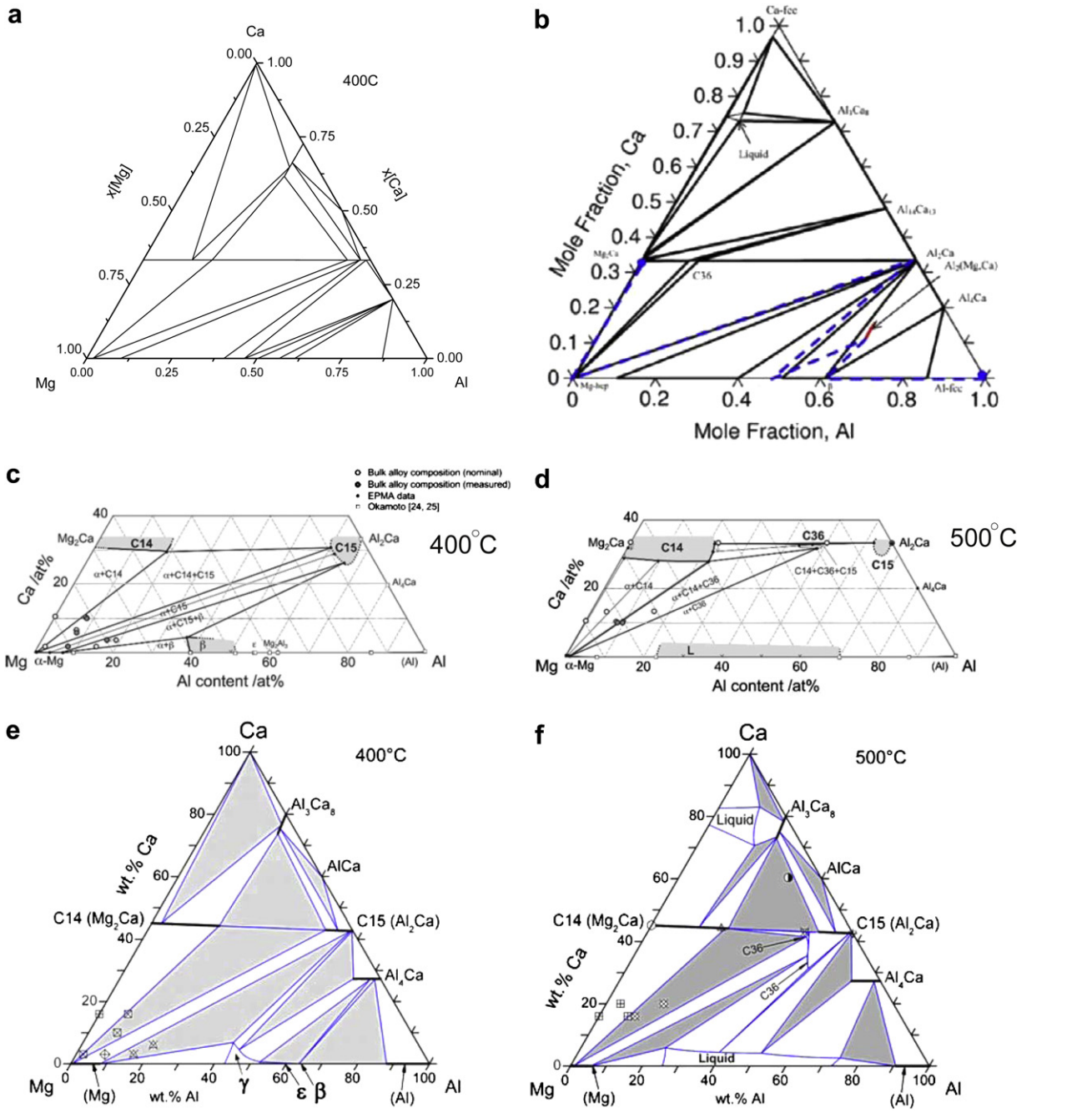

Fig. 1. Mg–Al–Ca isothermal sections from the literature: (a) at 400 °C [7], (b) at 415 °C [5], (c) at 400 °C [4], (d) at 500 °C [4], (e) at 400 °C [2] and (f) at 500 °C [2].

binary phases from Al–Ca system reported by [7] (Al_3Ca_8 and $Al_{14}Ca_{13}$) were not considered. Later, Ozturk [10] reinvestigated the Mg–Al–Ca ternary phase diagram as a part of the multicomponent Mg–Al–Ca–Sr system with a new model for the binary Al–Ca system that included the Al_3Ca_8 and the $Al_{14}Ca_{13}$ intermetallic compounds. Tkachenko et al. [11] also published their experimental work on this system. They studied the Mg–Al–Ca system in the Mg-rich corner and reported an isothermal section at 150 °C.

Luo et al. [12] suggested the presence of a ternary solid solution $(Mg,Al)_2Ca$ which is responsible for the improved creep resistance of Mg–Al–Ca alloys up to 200 °C due to its metallurgical stability and interfacial coherency with magnesium matrix. Its crystal structure was determined by Amerioun et al. [13] by single crystal x-ray diffractometry. They studied single crystals of this phase extracted from slow cooled samples and reported the existence of C36-Laves phase between Mg_2Ca and Al_2Ca with the composition range of $Mg_xAl_{(1-x)}Ca$ ($0.66 < x < 1.07$). Further, Suzuki et al. [3] reported in 2004 the existence of $(Al,Mg)_2Ca$ ternary intermetallic compound with the C36 crystal structure in an as-cast AXJ530 alloy (Mg–5Al–3Ca–0.15Sr, wt.%). In a later study of the Mg-rich alloys (in 2005), Suzuki et al. [14] reported that this C36 phase has a chemical composition of $Mg_{52}Al_{30}Ca_{18}$ and exists only at high temperature as a stable phase, but transforms to Mg and Al_2Ca at 300 °C. However, Suzuki et al. in 2006 [4] reported the composition of C36 phase as $Mg_{22}Al_{45}Ca_{33}$, which is different from [14]. Also, [4] reported that C36 compound forms during the eutectic reaction $L \leftrightarrow Mg + C36 + Mg_2Ca$ supporting their previous finding [14], but the temperature range of the C36 phase was changed. As illustrated

in Fig. 1(c) and (d), [14] has reported that the C36 phase with a wide homogeneity range is stable at 500 °C, but does not exist at 400 °C. It should be mentioned that the samples studied by Suzuki et al. [4] at 400 and 500 °C have different compositions. Only Mg-rich samples were studied at 400 °C, whereas samples studied at 500 °C have a wide range of compositions. According to the EPMA data reported by [4], the C36 phase was found only in samples with a high content of Ca and Al at 500 °C. The Mg-rich samples do not contain C36 phase neither at 400 °C nor at 500 °C. Additionally, [4] reported extensive solid solubilities of the Mg_2Ca, C36, $Al_{12}Mg_{17}$ and Al_2Ca phases as shown in Fig. 1(c) and (d).

Zhong et al. [5] reported a new $Al_2(Mg,Ca)$ solution found in a Mg_2Ca-Al diffusion couple at 415 °C. They analyzed this phase using SEM, EPMA, orientation imaging microscopy (OIM) and scanning transmission electron microscopy (STEM) combined with first-principle calculations and found that it is the C36 Laves phase with the lattice parameters a = 5.450Å and c = 17.514 Å. The isothermal section at 415 °C along with the diffusion path of the Mg_2Ca-Al diffusion couple are presented in Fig. 1(b).

Wang [15] investigated twenty-one as-cast alloys in this system using DSC, XRD and metallography. The thermal arrests were presented as well as the phase analysis of the as-cast and slow-cooled samples. Aljarrah et al. [16] re-assessed Wang's work and suggested the existence of extended solubilities for the Al_2Ca, Mg_2Ca and Al_3Ca_8 binary compounds, but no exact information on the phase boundaries was given.

Janz et al. [2] published a thermodynamic model of the Mg–Al–Ca system based on literature data and four key experiments. Similarly to [4] this thermodynamic model suggests that the C36 phase is stable at 500 °C, but does not exist at 400 °C. But according to [2] the composition of the C36 phase is different than that reported by [4], and as shown in Fig. 1(e) and (f), the homogeneity range of C36 at 500 °C extends in a different and quite unusual direction. Wide solid solubilities were also reported for the Al_2Ca, Al_4Ca, Mg_2Ca and Al_3Ca_8 binary compounds.

Several thermodynamic models were proposed in literature. Aljarrah et al. [16] and Islam et al. [17] reported thermodynamic models for the Mg–Al–Ca ternary system without modeling the ternary solid solutions and ternary phases. The more advanced models that included ternary solid solubilities of binary phases were reported by Gröbner et al. [7] and Ozturk [10]. The ternary $(Al,Mg)_2Ca$ C36-Laves phase was included in the models of Zhong et al. [5] and Janz et al. [2]. But its composition and homogeneity region do not correspond to the experimental data reported by Suzuki et al. [4] and Amerioun et al. [13]. There is no thermodynamic model that includes the $Al_2(Mg,Ca)$ phase C36-Laves phase.

3. Experimental

The alloys for diffusion couples and key experiments were prepared at MTL-CANMET from pure metals (Mg-99.8 wt.%, Al-99.9 wt.%, Ca-99 wt.%). CO_2-1%SF_6 gas was used as a protective atmosphere.

The solid–solid diffusion couples were prepared from two blocks of alloys and/or pure metals. The blocks' facing surfaces were pre-grinded up to 1200 grit using SiC paper and polished up to 1 μm using diamond paste and 99% ethanol as a lubricant. The blocks were pressed together using clamping rings, placed in a Ta container and sealed in a quartz tube under protective Ar atmosphere. The prepared samples were annealed at 400 °C for 2 weeks.

When, the solid–solid diffusion couples failed, solid–liquid diffusion couples were prepared instead. The block of alloy or metal with the lower melting temperature was melted on top of the block with the higher melting temperature in an arc-melting furnace under protective Ar atmosphere. The prepared samples were annealed at 400 °C for 2 weeks in a sealed quartz tube.

The annealed samples were grinded and polished up to 1 μm with 99% ethanol as a lubricant. The prepared samples were studied at CANMET by EPMA analysis using point and line scans. The two key samples were also studied by X-ray diffraction. The XRD patterns were obtained using PANanalytical Xpert Pro powder x-ray diffractometer with a CuKα radiation. The XRD spectrum was taken from 20 to 120 degree 2θ with a step size 0.02 degree 2θ and a scanning time 14s/step. X-ray diffraction study of the samples was done using X'Pert HighScore Plus Rietveld analysis software. The error of the EPMA measurements was estimated to be ~2 at.%. This value was obtained from the comparison and statistical analysis of the compositions of selected phases from several samples.

4. Results

As discussed above, although the Mg–Al–Ca system was studied by several authors, there are still many unsolved questions. This system contains four Laves phases: Mg_2Ca (C14, $MgZn_2$-structure type), Al_2Ca (C15, Cu_2Mg-structure type), $(Al,Mg)_2Ca$ (C36, $MgNi_2$-structure type) and $Al_2(Mg,Ca)$ (C36, $MgNi_2$-structure type). All these Laves phases have wide ranges of homogeneity, but literature data on their compositions and phase boundaries are contradictory. Additionally, the phase equilibria among these phases should be verified. In this work, we present experimental investigation of the compositions and phase boundaries of the Laves phases in the Mg–Al–Ca system in order to construct the isothermal section at 400 °C.

4.1. Diffusion couples study

4.1.1. The Mg–Ca diffusion couple

In the recent publication of Suzuki et al. [4], they reported extensive solubilities of the Al_2Ca and Mg_2Ca phases as illustrated in Fig. 1(c) and (d). They claimed that the Mg_2Ca phase has a solid solubility range around 5 at.% even in the binary Mg–Ca system. Since these data contradict previous studies of the Mg–Ca system, we have prepared a solid–solid Mg–Ca diffusion couple at 400 °C to determine the solubility limits of the Mg_2Ca phase. Despite of the successful formation of a Mg_2Ca diffusion layer, it cracked and chipped out during the metallographic preparation because of the brittleness of the Mg_2Ca diffusion layer. Therefore, solid–liquid Mg–Ca diffusion couple was prepared, resulting in a massive Mg_2Ca diffusion layer. The microstructure of the solid–liquid Mg–Ca and the EPMA line scans are presented in Fig. 2. Binary solid–liquid diffusion couples, in contrast to solid–solid ones, always contain two-phase region between the diffusion layers and the liquid end-member. In this diffusion couple, Mg was the liquid end-member and thus the $(Mg + Mg_2Ca)$ eutectic region was formed between the Mg and Mg_2Ca layers.

The results of the EPMA line scan of the solid–liquid Mg–Ca diffusion couple at 400 °C are shown in Fig. 2(b). Scan-2 in Fig. 2(a) is 600 μm long and contains 30 points. Three zones were identified in the diffusion couple: Mg, $(Mg + Mg_2Ca)$ eutectic and Mg_2Ca.

To determine the solubility range of the Mg_2Ca phase, a least squares approximation was applied for the points that correspond to the Mg_2Ca layer. As illustrated in Fig. 3, this least squares approximation has shown minimal composition variation of the Mg_2Ca phase. The standard deviation for Mg and Ca contents was found to be 1.3 at% and therefore the variation of the least squares approximation is within the error limits of EPMA measurement that was estimated as ~2 at.%. The solid solubility range of the Mg_2Ca binary phase calculated from the equation obtained by the

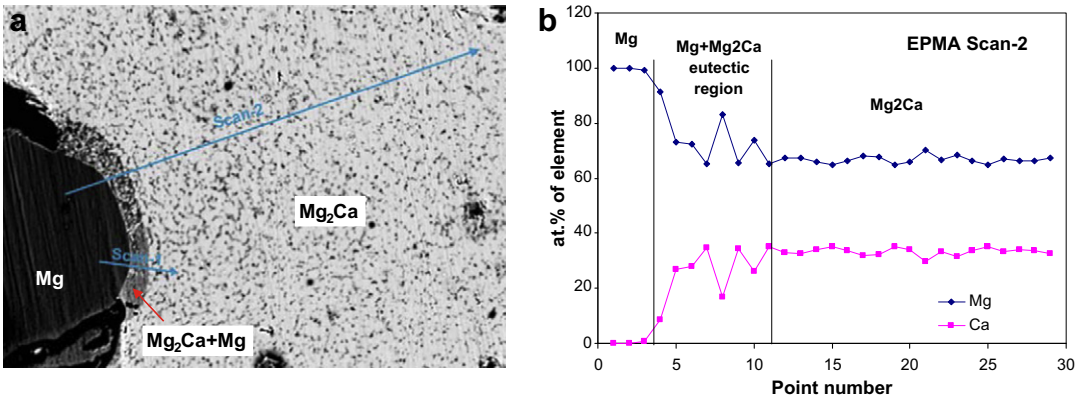

Fig. 2. (a) Microstructure of the solid–liquid Mg–Ca diffusion couple at 400 °C and EPMA line scans (b) EPMA analysis of line scan 2.

least squares approximation is 0.51 at.% Mg and consequently Mg_2Ca binary phase should be considered as stoichiometric.

4.1.2. The Al–Mg–Ca solid–solid diffusion couples

For precise analysis of the solid solutions in the Al–Mg–Ca system three solid–solid diffusion couples were prepared. Only the $(Mg_{29}Ca_{71})$–Al diffusion couple was successful. The $(Mg_{67}Ca_{33})$–$(Al_{67}Ca_{33})$ and the $(Al_{67}Mg_{33})$–$(Al_{67}Ca_{33})$ diffusion couples failed because of the high brittleness of the $Mg_{67}Ca_{33}$ and $Al_{67}Mg_{33}$ alloys that caused numerous cracks in the samples and prevented formation of diffusion layers.

A micrograph of the $(Mg_{29}Ca_{71})$–Al diffusion couple at 400 °C is shown in Fig. 4(a). This diffusion couple was made to determine the phase relations in the Al-rich corner and the center of the Al–Mg–Ca system. The composition profile of the $(Mg_{29}Ca_{71})$–Al diffusion couple annealed at 400 °C is illustrated in Fig. 4(b).

The diffusion path starts in a two phase $Mg_{29}Ca_{71}$ binary alloy; next is the area were the Ca-rich ternary eutectic region with the composition 18.0 ± 1.6 at.% Mg, 2.7 ± 0.2 at.% Al, 79.3 ± 1.5 at.% Ca is in equilibrium with the Al_3Ca_8 phase. The diffusion path crosses the Mg_2Ca phase and then goes to the $Mg_2Ca + Mg$ two phase region. Since the diffusion path crosses the Mg_2Ca solid solution perpendicular to the Mg_2Ca–Al_2Ca line, it indicates the substitution of Ca by Mg or Al. As could be seen from Figs. 4(b) and 5, the Mg_2Ca layer demonstrates no variation of the Ca composition and thus there is no substitution of Ca by Mg or Al in the Mg_2Ca solid solution. Next, the diffusion path crosses the $Al_2Ca + Mg$ two phase region and goes to the Al_2Ca solid solution. Al_2Ca phase demonstrates substitutional solid solubility, where Ca is substituted by Mg. The $Al_2(Ca,Mg)$ also has substitutional solid solubility as Ca is substituted by Mg atoms at constant 67 at.% Al. From the $Al_2(Ca,Mg)$ phase the diffusion path goes to the Al_4Ca phase, which has no ternary solid solubility. The last layer in this diffusion couple is the Al solid solution dissolving up to 2.8 at% Mg.

4.1.3. Key experiments

Since the $(Mg_{67}Ca_{33})$–$(Al_{67}Ca_{33})$ and the $(Al_{67}Mg_{33})$–$(Al_{67}Ca_{33})$ diffusion couples failed, two ternary key samples were prepared to determine the phase boundaries of the ternary $(Al,Mg)_2Ca$ and $(Al,Mg)_2Ca$ Laves phases. The prepared samples were annealed at 400 °C for 15 days and studied by EPMA and XRD.

The first key sample (KS1) was prepared to determine the homogeneity range of the $(Al,Mg)_2Ca$-C36 phase. The annealed KS1 alloy has a peritectic microstructure as presented in Fig. 6. The $(Al,Mg)_2Ca$ phase is formed between Mg_2Ca and Al_2Ca phases in such a way that it could be treated as a micro-diffusion couple. Therefore, two line scans (Fig. 6) were performed to determine the homogeneity regions of the Mg_2Ca, $(Al,Mg)_2Ca$ and Al_2Ca phases.

The first line scan, denoted as Scan-1 in Fig. 6, is 27 μm long and contains 20 points. Its composition profile is shown in Fig. 7(a). The second line scan, denoted as Scan-2 in Fig. 6, is 50 μm long and contains 25 points. Its composition profile is shown in Fig. 7(b).

Analysis of the EPMA data obtained from the KS1 alloy allowed us to determine the homogeneity range of the Mg_2Ca, $(Al,Mg)_2Ca$ and Al_2Ca phases along the Mg_2Ca–Al_2Ca joint (Fig. 8). The experimentally determined phase boundaries for these phases are given in Table 1. The estimated error of measurement is ~2 at.% Mg.

In order to verify our EPMA findings, KS1 was studied by XRD using X'Pert HighScore Plus Rietveld analysis software. XRD pattern illustrated in Fig. 9 demonstrates sharp peaks for the Mg_2Ca (○) and Al_2Ca (□) phases. The peaks of the $(Al,Mg)_2Ca$ phase (Δ) are extremely broad suggesting the existence of a wide homogeneity range. This supports our EPMA data as discussed above.

Broad peaks of the $(Al,Mg)_2Ca$ phase did not allow us to obtain a good agreement indices ($R_{exp} = 13.9$, $R = 28.0$, $R_w = 37.97818$, $GOF = 7.36101$), but using the Rietveld analysis with small values for the profile parameters we were able to determine lattice parameters of the phases at the phase boundaries (Fig. 9). The determined lattice parameters are presented in Table 2. They correspond to the compositions of the phase boundaries in Table 1.

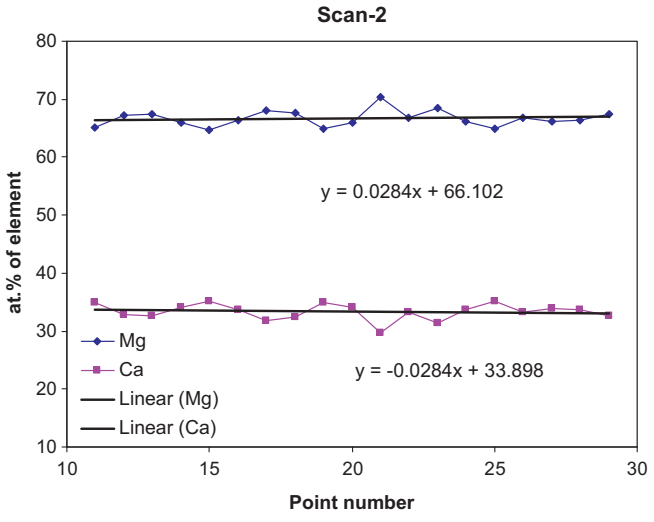

Fig. 3. Least squares approximation of the EPMA data of the Mg_2Ca layer.

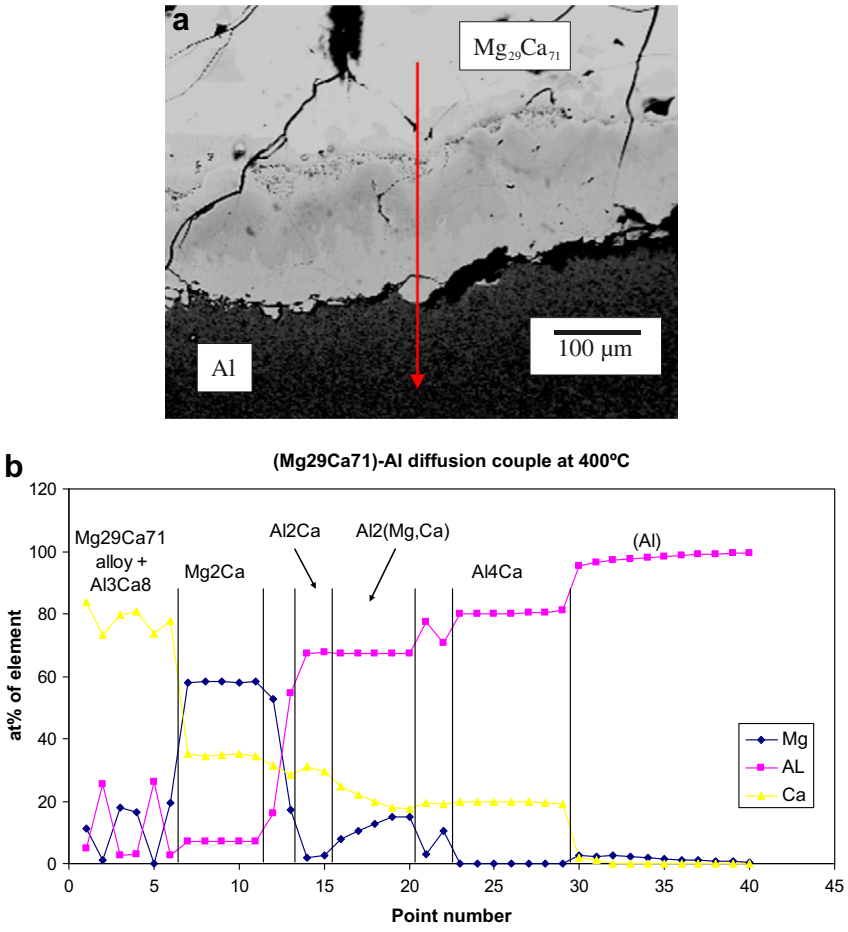

Fig. 4. (a) Micrographs of the ($Mg_{29}Ca_{71}$)-Al diffusion couple annealed at 400 °C, (b) Composition profile of the ($Mg_{29}Ca_{71}$)-Al diffusion couple.

The second key sample (KS2) was prepared to determine the homogeneity range of the Al_2(Ca,Mg)-C36 phase. The microstructure of the annealed KS2 alloy is presented in Fig. 10(a). It contains four different phases and therefore did not reach the global equilibrium, but the layers formed between the Al_2Ca and Al phases could be treated as a micro-diffusion couple with a local equilibrium between the layers. Two EPMA line scans were made to determine homogeneity regions of the Al_2Ca and Al_2(Ca,Mg) phases. The first line scan, denoted as Scan-1 on Fig. 10(a) is 90 μm long and contains 45 points. It crosses all four phases available in the sample: Al_2Ca, Al_2(Ca,Mg), $Al_{140}Mg_{89}$ and (Al). Its composition profile is shown in Fig. 10(b). The second line scan was made to determine more precisely the phase boundaries of the Al_2(Ca,Mg). It is 40 μm long and contains 20 points. Its composition profile is shown in Fig. 10(c).

Experimental data from both line scans were analyzed and presented in Fig. 11. In this figure, the points that belong to a single phase region were superimposed on the Gibbs triangle and the homogeneity regions of the ternary compounds were determined.

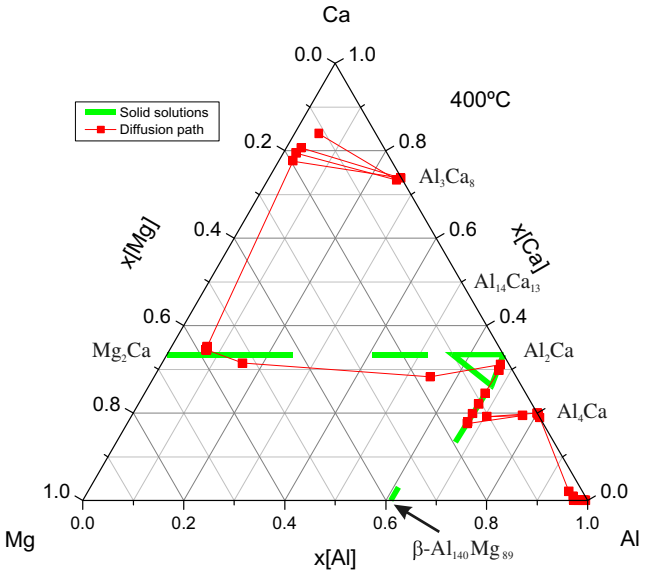

Fig. 5. Diffusion path of the ($Mg_{29}Ca_{71}$)-Al diffusion couple at 400 °C.

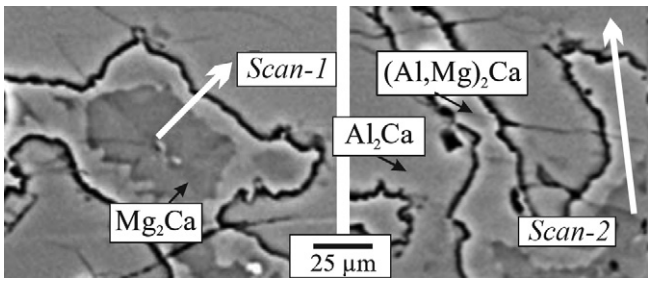

Fig. 6. Micrograph of the KS1 sample annealed at 400 °C for 15 days.

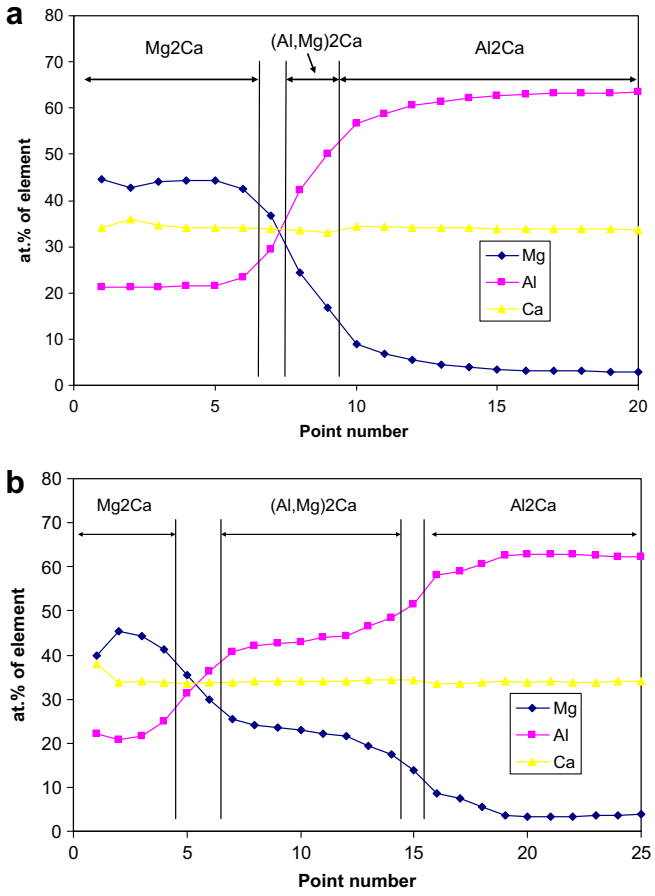

Fig. 7. (a) Composition profile of the 1st line scan in KS1 alloy, (b) Composition profile of the 2nd line scan in KS1 alloy.

The solubility ranges of the Al_2Ca, $Al_2(Ca,Mg)$, $Al_{140}Mg_{89}$ and (Al) phases are presented in Table 3. The estimated error of measurement is ~2 at/% Al.

The XRD pattern is illustrated in Fig. 12. It demonstrates the Rietveld analysis for the Al_2Ca, $Al_2(Ca,Mg)$, $Al_{140}Mg_{89}$ and (Al) phases in the KS2 sample. Silicon peaks appear in this spectrum because it is used as an internal standard. The determined lattice parameters of the phases are presented in Table 4. They correspond to the compositions of the phase boundaries in Table 3.

4.1.4. *Mg–Al_2Ca liquid–solid diffusion couple*

In order to determine phase relations between the Mg and Al_2Ca phases, a liquid-solid diffusion couple was prepared and annealed at 400 °C for two weeks. No continuous diffusion layers were formed in this diffusion couple. As shown in Fig. 13, three diffusion

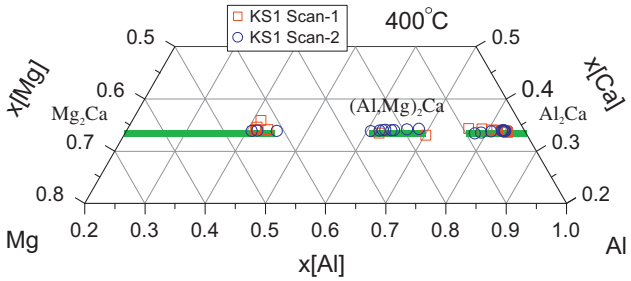

Fig. 8. Homogeneity regions of the Mg_2Ca, $(Al,Mg)_2Ca$ and Al_2Ca phases.

Table 1
Experimentally determined phase boundaries of the Mg_2Ca, $(Al,Mg)_2Ca$ and Al_2Ca phases along the Al_2Ca–Mg_2Ca join at 400 °C.

Phase	Phase boundaries, at.% Al/Ca/Mg	
	Start	End
Mg_2Ca	0/33.33/66.67[a]	24.91/33.33/41.76
$(Al,Mg)_2Ca$	40.61/33.33/26.06	48.39/33.33/18.28
Al_2Ca	57.66/33.33/9.01	66.67/33.33/0[a]

[a] Value is calculated from the stoichiometry of the phase.

zones were formed between Al_2Ca and Mg alloys. The zones ***a*** and ***c*** represent the mixture of (Mg–Al_2Ca) eutectic with Al_2Ca and Mg dendrites respectively. The zones ***b*** represents the region of fine globular (Mg–Al_2Ca) eutectic. Only Mg and Al_2Ca phases were found in this diffusion couple. That means that the Mg and the Al_2Ca phases form a stable two-phase region at 400 °C. The Mg–Al_2Ca tie-line was obtained by the EPMA analysis of the Mg and phases near the phase boundaries. The composition of Mg was found to be 97.5 ± 1.1 at.% Mg, 2.0 ± 0.6 at.% Al and 0.4 ± 0.5 at.% Ca. The Al_2Ca composition was found to be 3.2 ± 0.5 at.% Mg, 64.1 ± 0.5 at.% Al and 32.7 ± 0.3 at.% Ca.

5. Discussion

The main issue in the Mg–Al–Ca system is the precise determination of the solid solution boundaries. Therefore, the experimental data on solid solubility and phase relations for the Mg_2Ca, $(Al,Mg)_2Ca$, Al_2Ca, Al_4Ca, $Al_2(Ca,Mg)$, $Al_{140}Mg_{89}$ and (Al) phases were collected and analyzed. The Mg_2Ca, $(Al,Mg)_2Ca$, $Al_2(Ca,Mg)$ phases have unidirectional solid solutions with wide homogeneity ranges. The $Al_{140}Mg_{89}$ compound also has unidirectional solid solution, but the homogeneity range is limited to 3 at.% Ca. No ternary solubility was detected for the Al_4Ca compound. The Al_2Ca phase has a complex area of homogeneity that is illustrated in Fig. 14.

The shape of the Al_2Ca solution at 400 °C, defined by EPMA data, indicates that Mg substitute both Al and Ca. The determined homogeneity range is in good agreement with EPMA data reported by [4]. The analysis of the lattice parameters showed that

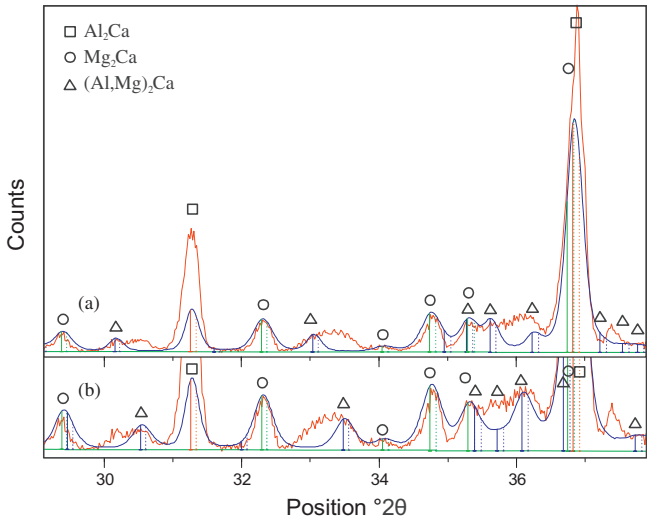

Fig. 9. Rietveld analysis for the key sample KS1 annealed at 400 °C for 15 days. It contains Mg_2Ca (○), Al_2Ca (□) and $(Al,Mg)_2Ca$ (Δ) phases. (a) – Mg-rich pattern of the $(Al,Mg)_2Ca$ phase, (b) – Al-rich pattern of the $(Al,Mg)_2Ca$ phase.

Table 2
Lattice parameters of the Mg_2Ca, $(Al,Mg)_2Ca$ and Al_2Ca phases.

Phase	Space group (No.)	Lattice parameters at phase boundaries, Å	
		Start	End
Mg_2Ca	P 63/m m c (194)	a = 6.2709(5)[a] c = 10.1696(7)[a]	a = 6.079(1), c = 9.778(3)
$(Al,Mg)_2Ca$	P 63/m m c (194)	a = 5.925(1), c = 19.155(9)	a = 5.854(2), c = 19.06(1)
Al_2Ca	F d-3 m (227)	a = 8.0900(4)	a = 8.022[a]

[a] Data obtained from the [18].

substitution of Al by Mg increases the lattice parameter ***a*** from 8.022 to 8.090 Å (see Tables 1 and 2). In contrast, the substitution of Al by Mg decreases the lattice parameter ***a*** from 8.022 to 8.011 Å (see Tables 1 and 2).

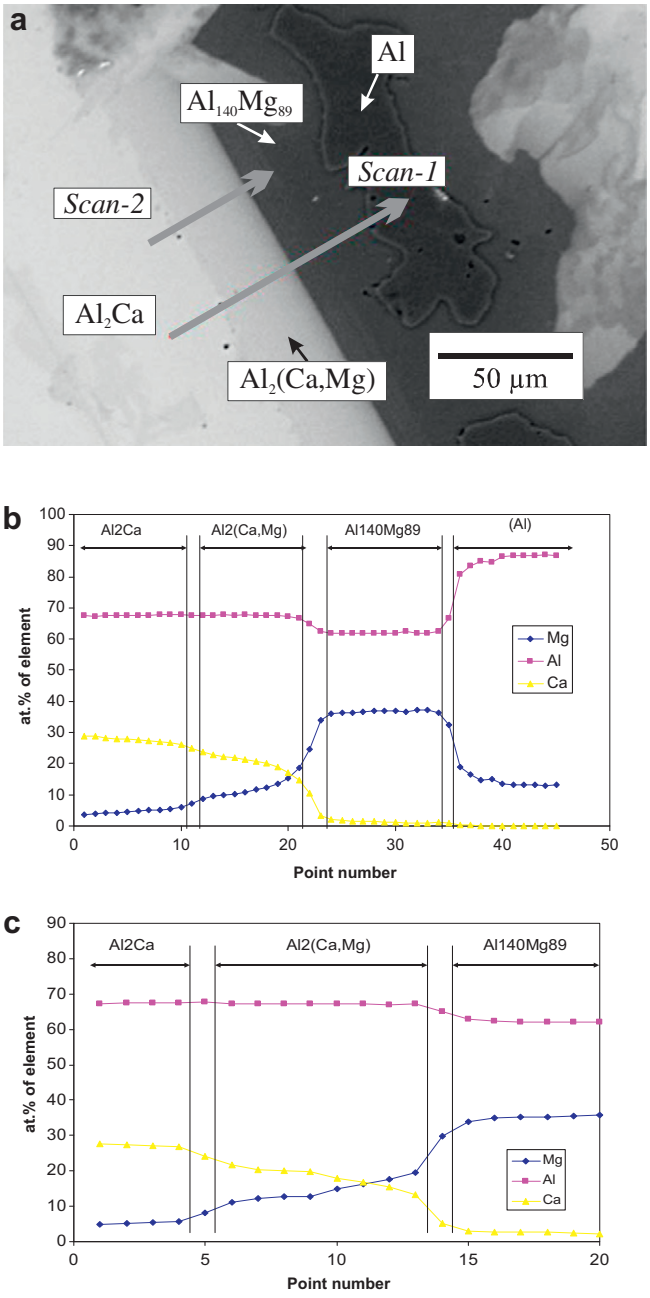

Fig. 10. (a) Micrograph of the KS2 sample annealed at 400 °C for 15 days, (b) Concentration profile of the 1st line scan and (c) Concentration profile of the 2nd line scan.

Such behavior is understandable considering the atomic sizes of elements. According to [19] the empirical metallic radii of Al, Mg and Ca are 1.25, 1.50 and 1.80 Å, respectively. Thus, the difference between Al and Mg atoms is 0.25 Å and the difference between Mg and Ca atoms is 0.3 Å. The small difference in atomic sizes allows Mg to substitute both Al and Ca atoms. Since the difference between Al and Mg atoms is smaller, the substitution between Al and Mg is higher (9.01 at.%) than the substitution between Mg and Ca (5.92 at.%).

The experimental data for all other phases were also carefully analyzed and compared with the literature data as shown in Fig. 15.

The Mg_2Ca solid solution was studied using binary and ternary samples. It extends in the ternary system as a substitutional solid solution where Mg atoms are substituted by Al up to 24.91 at.% Al. No substitution between Mg and Ca atoms was found. This finding agrees well with the data of [2,5,7,13] who also reported a unidirectional solubility and similar ternary extension of the solid solution. The area shaped solubility of the Mg_2Ca solid solution reported by [4] (Fig. 1(c) and (d)) is based on one experimental point obtained from the Mg-rich sample that gives the composition $Al_{18.9}Ca_{29.5}Mg_{51.6}$ to Mg_2Ca phase (Fig. 15). Since the EPMA analysis was done for Mg-rich samples only, it is possible that the spot could catch Mg-matrix and therefore the composition of the Mg_2Ca phase is shifted towards Mg.

The literature data on the $(Al,Mg)_2Ca$-C36 phase are the most controversial. As described in our literature review and presented in Fig. 1, the authors of [2,4,5,13,14] completely disagree with each other on the composition and the solubility range of this compound. Unfortunately, most authors studied slow-cooled and as-cast alloys. Only [4,14] studied samples annealed at 400 and 500 °C and reported that C36 is a high-temperature phase that decomposes below 500 °C. But, as could be seen in Fig. 1(c) and (d), only Mg-rich samples were studied at 400 °C. Careful analysis of the EPMA data reported by [4] showed that the $(Al,Mg)_2Ca$-C36

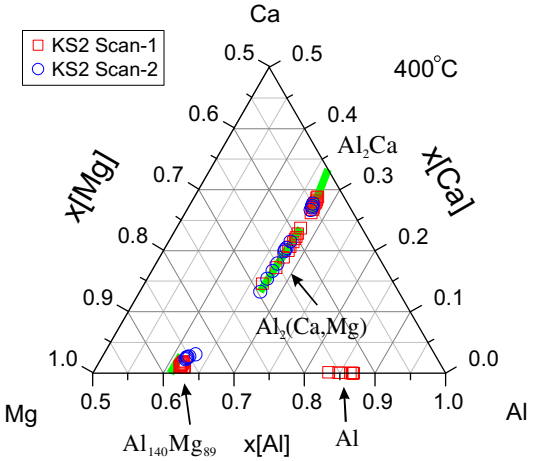

Fig. 11. Homogeneity regions of the Al_2Ca, $Al_2(Ca,Mg)$, $Al_{140}Mg_{89}$ and (Al) phases.

Table 3
Experimentally determined phase boundaries at 400 °C of the Al_2Ca, $Al_2(Ca,Mg)$, $Al_{140}Mg_{89}$ and (Al) phases

Phase	Phase boundaries, at.% Al/Ca/Mg	
	Start	End
Al_2Ca	66.67/33.33/0	67.81/26.27/5.92
$Al_2(Ca,Mg)$	67.6/23.74/8.67	67.13/13.3/19.57
β-$Al_{140}Mg_{89}$	62.03/3.07/32.90	61.14/0/38.86[a]
(Al).	83.34/0.15/16.51	100/0/0[a]

[a] Value is calculated from the stoichiometry of the phase.

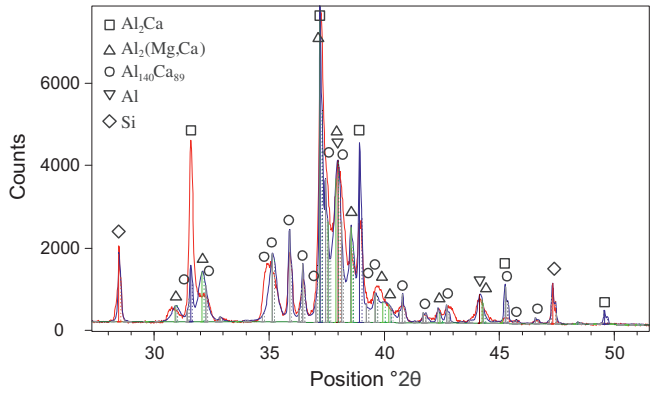

Fig. 12. Rietveld analysis for key sample KS2 annealed at 400 °C for 15 days.

phase was found at 500 °C in the samples that contain more than 10 at.% Ca and 9.7 at.% Al. The $(Al,Mg)_2Ca$-C36 phase was not found in the Mg-rich samples at both temperatures. Since, Suzuki et al. [14,4] did not study any samples close to the $(Al,Mg)_2Ca$ composition at 400 °C, Mg-rich samples can not be used as a solid evidence that C36 phase is not stable at 400 °C.

Besides, [2] reported a thermodynamic model where $(Al,Mg)_2Ca$-C36 phase is not stable at 400 °C (Fig. 1(e) and (f)), despite their own finding that the C36 phase is present in the slow cooled $Al_{47.53}Ca_{33.2}Mg_{19.3}$ alloy. The composition of the C36 phase found in this alloy is $Al_{44.9}Ca_{32.5}Mg_{22.5}$ that is in a good agreement with our data (Fig. 15). The freezing temperature of the slow-cooled $Al_{47.53}Ca_{33.2}Mg_{19.3}$ alloy [2] should be lower than 400 °C, because the ternary extension of the Mg_2Ca and Al_2Ca solid solutions in this sample are smaller than in KS1 sample annealed at 400 °C (Fig. 15). Therefore, we can use the data of [2] as an indirect evidence of the fact that $(Al,Mg)_2Ca$ phase is stable at 400 °C. Also [13] found the $(Al,Mg)_2Ca$-C36 phase in slow-cooled samples. They found sufficient amount of this phase to extract single crystals from the samples that were cooled at 20 °C/h. Such a slow cooling rate should cause full decomposition of the C36 phase if assumed that it decomposes between 400 and 500 °C. In this work, the $(Al,Mg)_2Ca$ phase was found in the as-cast and in the alloys annealed for 2 weeks at 400 °C. Based on this discussion and presented experimental data, we suggest that $(Al,Mg)_2Ca$-C36 phase is stable at 400 °C.

The composition $(Al,Mg)_2Ca$ phase found in this work (Table 1) agrees well with the compositions reported by [4] for 500 °C and, [13] and [2] for slow-cooled alloys. But in contrast to [4], [13] and [2] who made a single point analysis, we have analyzed samples

Table 4
Lattice parameters of the Al_2Ca, $Al_2(Ca,Mg)$, $Al_{140}Mg_{89}$ and (Al) phases.

Phase	Space group (No.)	Lattice parameters at phase boundaries, Å	
		Start	End
Al_2Ca	F d -3 m (227)	a = 8.022[a]	a = 8.0116(2)
$Al_2(Ca,Mg)$	P 6_3/m m c (194)	a = 5.58, c = 18.05[b]	a = 5.58, c = 18.05[b]
$Al_{140}Mg_{89}$	F d -3 m (227)	a = 28.3126(8)	a = 28.2435(1)[a]
(Al).	F m -3 m (225)	a = 4.1013(3)	a = 4.049750(15)[a]

[a] Data obtained from the [18].
[b] Average value.

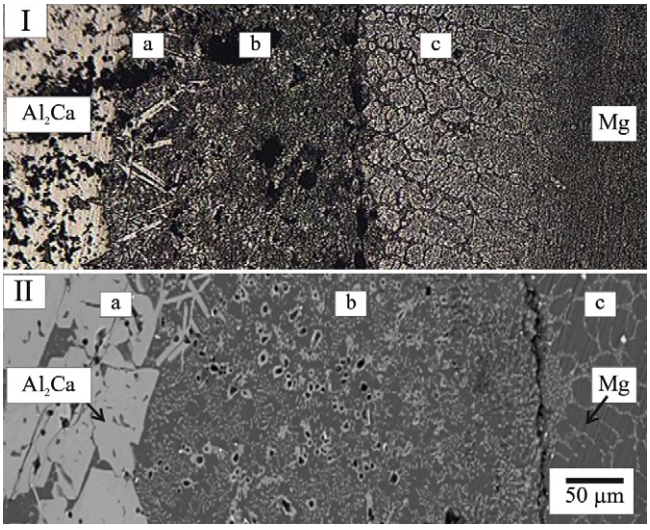

Fig. 13. Mg–Al_2Ca liquid–solid diffusion couple at 400 °C. (I) Optical micrograph. (II) BSE micrograph. (a) – Al_2Ca dendrites + (Mg–Al_2Ca) eutectic; (b) – (Mg–Al_2Ca) eutectic; (c) – Mg dendrites + (Mg-Al_2Ca) eutectic.

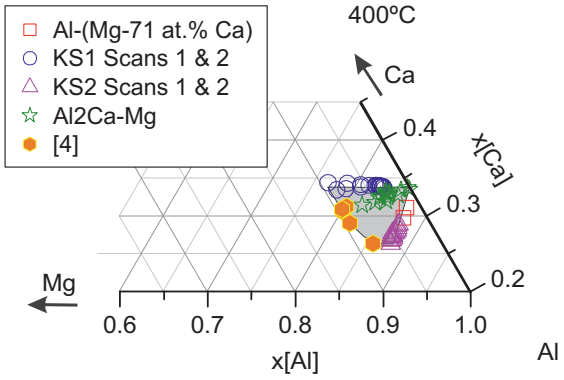

Fig. 14. Solubility limits of the Al_2Ca solid solution at 400 °C.

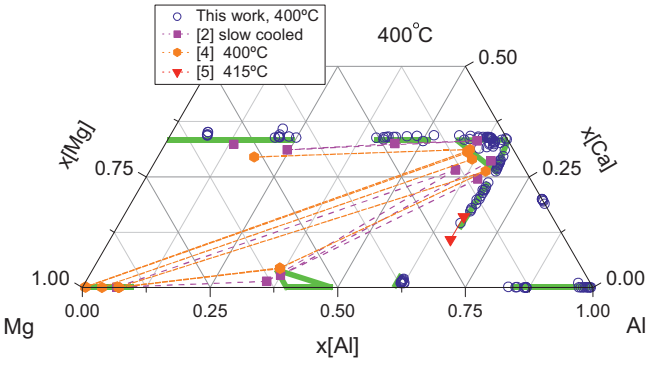

Fig. 15. EPMA results in relation to experimental data from the literature.

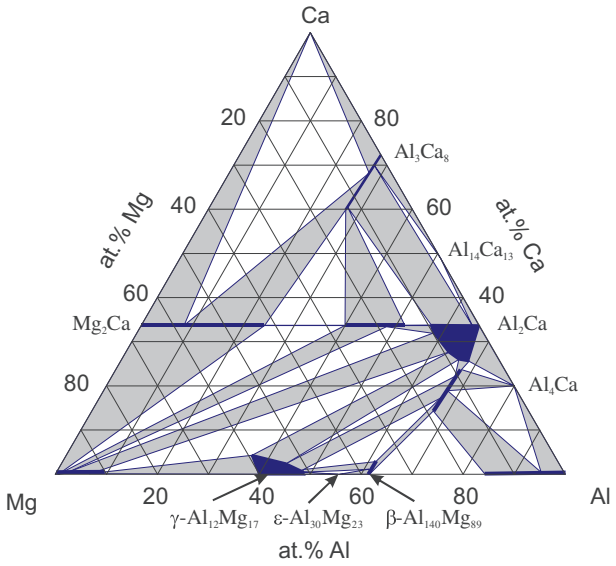

Fig. 16. Isothermal section of the Al-Mg-Ca phase diagram at 400 °C.

using the EPMA line scans that allowed us to determine complete homogeneity range of this compound.

The Al_2(Ca,Mg) is the second C36 phase in this system. It was reported first by Zhong et al. [5], who has determined Mg-rich boundary of this solid solution at 415 °C. No other authors reported this phase. In this work, the complete solubility range of the Al_2(Ca, Mg)-C36 at 400 °C was determined using EPMA line scan technique (Table 3). Its crystal structure was confirmed using X-ray powder diffraction. Our experimental results are in excellent agreement with the data of [5] and [2] reported the phase with the composition $Al_{65.2}Ca_{24.5}Mg_{10.3}$ in the slow-cooled $Al_{36.8}Ca_{4.5}Mg_{58.6}$ alloy (Fig. 15). They associated this composition with the Al_4Ca phase despite the fact that 25 at.% Ca can not correspond to substitutional solid solution of Al_4Ca, which must have 20 at.% Ca. This resulted in extending the Al_4Ca solid solution up to 10 at.% Mg as could be seen in Fig. 1(e) and (f). We suggest that this composition should be associated with the Ca-rich part of the Al_2(Ca,Mg)-C36 phase, as can be clearly seen in Fig. 15.

The Al_4Ca and $Al_{140}Mg_{89}$ phases were analyzed in addition to the Laves phases in this system. The Al_4Ca phase was analyzed as a part of the $(Mg_{29}Ca_{71})$-Al diffusion couple. As could be seen in Figs. 4(b) and 5, the Al_4Ca phase has no ternary solid solubility. The $Al_{140}Mg_{89}$ phase is a line-shaped solid solution with the homogeneity ranges up to 3 at.% Ca due to the substitution of Mg by Ca.

Based on the current experimental data, the isothermal section of the Al-Mg-Ca phase diagram at 400 °C has been constructed and presented in Fig. 16. The phases, solid solubility limits and phase equilibria were determined using the EPMA and XRD data.

6. Conclusion

The isothermal section of the Al–Mg–Ca phase diagram at 400 °C is constructed as a result of experimental study of the Mg–Al–Ca system. The $(Al,Mg)_2Ca$ and $Al_2(Mg,Ca)$ ternary Laves phases were found in this system. Their homogeneity ranges and crystal structures were obtained by EPMA and XRD analysis of the diffusion couples and ternary key samples. Also, the ternary solid solubilities for the Mg_2Ca, Al_2Ca, Al_4Ca, $Al_{140}Mg_{89}$ phases were determined. This study enhanced the understanding of the ternary Al–Mg–Ca phase diagram. It demonstrated that the phase relations and the solubility ranges of the phases are more complex than what was reported in the literature in terms of thermodynamic models and experimental studies.

Acknowledgments

Financial support from General Motors of Canada Ltd. and the Natural Sciences and Engineering Research Council of Canada (NSERC) through the CRD grant program is gratefully acknowledged.

References

[1] Luo AA. International Materials Reviews 2004;49(1):13.
[2] Janz A, Gröbner J, Cao H, Zhu J, Chang YA, Schmid-Fetzer R. Acta Materialia 2009;57:682.
[3] Suzuki A, Saddock ND, Jones JW, Pollock TM. Scripta Materialia 2004;51 (10):1005.
[4] Suzuki A, Saddock ND, Jones JW, Pollock TM. Metallurgical and Materials Transactions A 2006;37(A):975.
[5] Zhong Y, Liu J, Witt RA, Sohn YH, Kui Liu Z. Scripta Materilia 2006;55(6):573.
[6] Catterall JA, Pleasance RJ. Journal of Institute of Metals 1957;1817:189.
[7] Gröbner J, Kevorkov D, Chumak I, Schmid-Fetzer R. Z Metallkde 2003;94:976.
[8] Ozturk K, Yu Zhong, Liu ZK. In: Magnesium technology. US: TMS, The Minerals, Metals and Material Society; 2003. p. 113.
[9] Ozturk K, Zhong Y, Luo AA, Liu ZK. Research summary. High Temperature Magnesium 2003;55(11):40.
[10] Ozturk K. PhD thesis, The Pennsylvania State University, 2004.
[11] Tkachenko VG, Khoruzhaya VG, Meleshevich KA, Karpets MV, Frizel VV. Powder Metallurgy and Metal Ceramics 2003;42(5–6):268.
[12] Luo AA, Balogh MP, Powell BR. Tensile creep and microstructure of magnesium–aluminum–calcium based alloys for powertrain applications: Part 2 of 2. In: Society of Automotive Engineers, Light Metal Applications for the Automotive Industry: Aluminum and Magnesium; 2001. p. 37.
[13] Amerioun S, Simak SI, Haeussermann U. Inorganic Chemistry 2003;42 (5):1467.
[14] Suzuki A, Saddock ND, Jones JW, Pollock TM. Acta Materillia 2005;53(9):2823.
[15] Wang XZ. Concordia University, Montreal, Canada, Masters Thesis, 2005.
[16] Aljarrah M, Medraj M, Wang X, Essadiqi E, Muntasar A, Denes G. Journal of Alloys and Compounds 2007;436:131.
[17] Islam F, Medraj M. Journal of the Canadian Metallurgical Quarterly 2005;44 (4):523.
[18] ICSD for WWW database http://wwwicsdiqfrcsices as for March 1, 2009.
[19] www.webelements.com as of March 1, 2009.